Visualizing Kinetically Robust $Co^{III}_4L_6$ Assemblies *In Vivo*: SPECT Imaging of the Encapsulated $[^{99m}Tc]TcO_4^-$ Anion

Benjamin P. Burke,[§,‡,‖] William Grantham,[§,†] Michael J. Burke,[§,†] Gary. S. Nichol,[†] David Roberts,[⊥,‖] Isaline Renard,[‡,‖] Rebecca Hargreaves,[‡,‖] Christopher Cawthorne,[⊥,‖] Stephen J. Archibald,*[,‡,‖] and Paul J. Lusby*[,†]

[†]EaStCHEM School of Chemistry, University of Edinburgh, Joseph Black Building, David Brewster Road, Edinburgh, Scotland EH9 3FJ.

[‡]Department of Chemistry, University of Hull, Cottingham Road, Hull, HU6 7RX, UK.

[⊥]School of Life Sciences, University of Hull, Cottingham Road, Hull, HU6 7RX, UK.

[‖]Positron Emission Tomography Research Centre, University of Hull, Cottingham Road, Hull, HU6 7RX, UK

Supporting Information Placeholder

ABSTRACT: Non-covalent encapsulation is an attractive approach for modifying the efficacy and physiochemical properties of both therapeutic and diagnostic species. Abiotic self-assembled constructs have shown promise, yet many hurdles between *in vitro* and (pre)clinical studies remain, not least the challenges associated with maintaining the macromolecular, hollow structure under non-equilibrium conditions. Using a kinetically robust $Co^{III}_4L_6$ tetrahedron we now show the feasibility of encapsulating the most widely used precursor in clinical nuclear diagnostic imaging, the gamma emitting $[^{99m}Tc]TcO_4^-$ anion, under conditions compatible with *in vivo* administration. Subsequent SPECT imaging of the caged-anion reveals a marked change in the biodistribution compared to the thyroid-accumulating free oxo-anion, thus moving clinical applications of (metallo)supramolecular species a step closer.

Technetium-99m (t½ = 6 hours) is a gamma emitting radioactive isotope used in >80% of clinical nuclear diagnostic imaging scans, with over 40 million single-photon emission computed tomography (SPECT) scans annually carried out worldwide.[1] The new generation of molecular imaging agents (including positron emission tomography (PET) tracers) target specific molecules associated with disease (e.g. enzymes, protein or other antigens), however, technetium-based imaging agents have generally utilized lipophilicity, charge or other non-molecular actions, often to determine tissue blood flow as an indirect measure of function.[2] Syntheses of molecular clinical imaging agents for SPECT involve reduction of the $[^{99m}Tc]TcO_4^-$ anion, which is eluted directly from a $^{99}Mo/^{99m}Tc$ generator. This can limit applications as the typical radiopharmaceutical kit must bring about *in situ* reduction of the +7 pertechnetate oxidation state, which can be difficult to control precisely and is often incompatible with chelator-biomolecule conjugates.[3] The reliance on a reductive approach to technetium-based imaging agents is due to the assumption that the *"chemical reactivity of the pertechnetate anion is negligible; it does not bind to any ligand*".[1a]

While pertechnetate encapsulation has been investigated for nuclear waste stream management,[4] similar chemistry has not been exploited for imaging agents. The speed and efficacy of non-covalent encapsulation, avoiding additional reagents, brings advantages because of the rapid decay of the radioisotope, and the need to provide a simple clinical kit. Cationic coordination tetrahedra are known to bind small anions,[5] thus encapsulation has the potential to break the paradigm that $[^{99m}Tc]TcO_4^-$ cannot be used directly in targeted molecular SPECT imaging. The relative small size and monodispersity of a coordination cage (< 3 kDa, 1-2 nM) also provides advantages over larger nanoscale carriers; it should be possible to develop these compounds for effective distribution in the vasculature, and to give clearance via renal excretion on an imaging timescale, a common problem with nanoparticle systems.[6] However, there are challenges with using self-assembled systems *in vivo* as most exist in an equilibrium state with their disassembled components.[7] This is less problematic for applications such as catalysis,[8] where intact species are typically favored. In contrast, *in vivo* conditions severely challenge equilibrium systems because of the low-concentration required for a safe dose and numerous competing "ligands".[9] This is particularly true for nuclear medicine applications, as the very high sensitivity and radioactivity means very small amounts (as low as nanograms) of the agent are usually administered.

Self-assembled coordination assemblies are known to possess interesting biological properties.[10] It has also been shown that host-guest chemistry can enhance *in vitro* cytotoxicity and improve cellular uptake.[11] However, *in vivo* investigations are extremely rare,[12] possibly due to concerns about structural integrity. Recently, we started to explore an "assembly-followed-by-fixing" method for generating robust assemblies. This involves post-assembly oxidation of dynamic Co^{II} species to give non-equilibrium Co^{III} analogues.[13] Moving this system forward, the development of an *in vivo* imaging agent utilizing $[^{99m}Tc]TcO_4^-$ encapsulation was an appealing option. The bio-distribution of

the free [^{99m}Tc]TcO_4^- anion is well known,[14] therefore any perturbation would validate the approach under pre-clinical conditions and by extension demonstrate the robustness of the system.

Initially, our investigation focused on the host-guest chemistry of the tetrahedral $[Co^{III}_4\mathbf{L^1}_6]\cdot 12NO_3$ (**C-1**·$12NO_3$, Figure 1a) in D_2O using "cold" anions. As expected, more "hydrophobic" anions bind best, with PF_6^- giving the highest K_a (91000 M^{-1}; see Supporting Information) while the pertechnetate analogue, perrhenate (ReO_4^-) also showed significant affinity (61000 M^{-1}). The binding of this anion is easy to observe due to slow exchange on the ^{1}H NMR timescale, with separate signals for the empty and occupied capsule at sub-stoichiometric ratios (Figure 2). Anions including BF_4^-, ClO_4^- and even SO_4^{2-} also bind, albeit more-weakly, with K_a ranging from 100 M^{-1} (SO_4^{2-}) to 7000 M^{-1} (ClO_4^-). The relative affinities of these anions is difficult to accurately rationalize due to the interplay of multiple factors, including size and shape complementary, coulombic attraction and de-solvation energies.[15] Considering other biological anions that might compete with a radiolabelled cage, we also examined PO_4^{3-}. This showed no evidence of binding in D_2O, presumably because of the increasing de-solvation penalty. The encapsulation of ClO_4^- has also been confirmed by X-ray crystallography (Figure 1b).

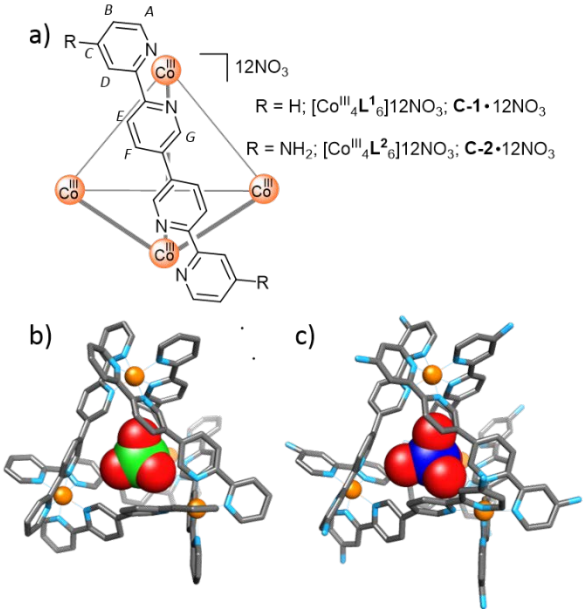

Figure 1. (a) Chemical structure of anion-binding $Co^{III}_4L_6$ cages (only one ligand shown for clarity); X-ray crystal structures of (b) [$ClO_4\subset$**C-1**]$^{11+}$; (c) [$ReO_4\subset$**C-2**]$^{11+}$. Non-encapsulated anions and solvent molecules removed for clarity. Color Code: Co, orange; C, grey; N, light blue; O, red; Cl, green; Re, dark blue.

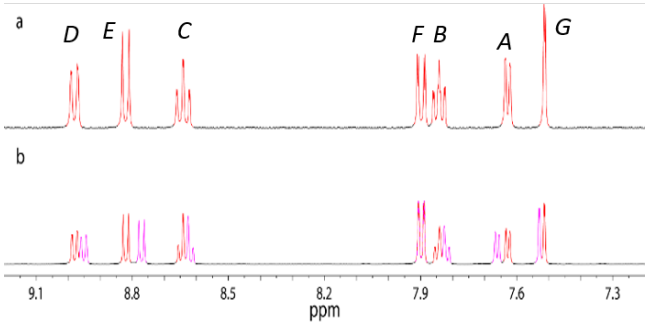

Figure 2. ^{1}H NMR spectra (500 MHz, D_2O, 298 K) showing the encapsulation of ReO_4^- by **C-1**$^{12+}$. (a) **C-1**·$12NO_3$ only; (b) **C-1**·$12NO_3$ + NH_4ReO_4 (free cage signals in red, occupied in pink). The assignments correspond to lettering shown in Figure 1a.

Turning to [^{99m}Tc]TcO_4^- encapsulation, we started by investigating the concentration of **C-1**$^{12+}$ required to give quantitative (>95%) radiochemical yield (RCY) of radio-labelled species, as this would dictate the minimum dose in subsequent *in vivo* imaging experiments. This was assessed using thin layer chromatography (TLC) on standard-phase silica gel; while free [^{99m}Tc]TcO_4^- elutes in water with the solvent front, encapsulated [$TcO_4\subset$**C-1**]$^{11+}$ is retained on the baseline. Analysing the TLC plates using a gamma counter showed that full encapsulation could be achieved at 100 μM **C-1**, with an EC_{50} (cage concentration required for 50% RCY) of 14 μM (Figure 3, black squares). These preliminary experiments also showed that, as anticipated, cage labelling using encapsulation is facile and rapid, with the RCY invariant of mixing time from 5 minutes to hours (data not shown).

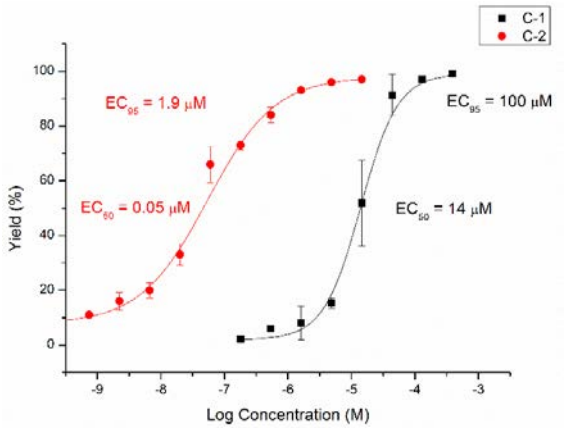

Figure 3. Radiochemical yield for [^{99m}Tc]TcO_4^- encapsulation as a function of cage concentration (**C-1**, black squares; **C-2**, red circles). For details see Supporting Information.

Next, the RCY was assessed under a range of conditions designed to probe the stability of the encapsulated species (Figure 4, grey bars). The RCY is maintained at a reasonable level (40-60%) after the addition of competing NO_3^-, $Cl^-$and $PO_4(H)^{2-/3-}$ anions that are relevant to *in vivo* use. In contrast, when anions which bind within **C-1** (i.e. ClO_4^- and PF_6^-) were added to the radiolabelled cage, the stability was negligible. While neither ClO_4^- nor PF_6^- represent concerns from an *in vivo* perspective, they show that the high RCY is due to encapsulation rather than simple ion-pairing with the cage periphery. Further controls with assemblies possessing both smaller and larger cavities (i.e., analogous $Co^{III}_2L_3$ and $Co^{III}_4L_6$ species[12b], see Supporting Information) showed no discernible binding at 100 μM, further demonstrating the complementary of **C-1** for the [^{99m}Tc]TcO_4^- anion. The stability experiments with competitive anions also show the RCY does not change as a function of time. In contrast, the same stability experiment carried out in serum showed a steady decrease in RCY, diminishing to negligible levels of intact host-guest system after 24 hours. As displacement by biological "guests" would likely be rapid, we attribute the slower release of the [^{99m}Tc]TcO_4^- anion to cage degradation, possibly facilitated by biological reductants (antioxidants). To test this, the reaction of **C-1** with excess glutathione was examined using ^{1}H NMR spectroscopy (Figure S6).[16] This showed the rapid disappearance of the diamagnetic signals of **C-1**, indicating a possible cage disassembly mechanism that involves initial reduction of some or all of the Co^{III} centers.

Considering structural modification to improve cage integrity in biological medium, we targeted stabilization of the +3 oxidation state. Reasoning that a stronger σ-donor ligand would achieve this, the novel 4-amino-2,2′-bipy analogue, **C-2**, was developed (Figure 1a). It was also envisaged that the more strongly coordinating $\mathbf{L^2}$ would also inhibit direct ligand substitution from either oxidation state. The diamino substituted ligand, $\mathbf{L^2}$, was synthesized in several steps, starting with nitration of 2-bromopyridine-*N*-oxide, followed by metal-catalyzed cross-coupling, then reduction and homo-coupling reactions (see Supporting Information). The enhanced ligand "strength" became immediately apparent when preparing **C-2**; equilibration of the Co^{II} precursor required prolonged microwave irradiation. Even then, oxidation yielded a mixture of **C-2** and the corresponding helicate $[Co^{III}_2\mathbf{L^2}_3]^{6+}$, which we attribute to probable kinetic trapping in the assembly phase of the reaction. Nonetheless, the smaller species could be removed using size-exclusion chromatography, which gave a pure sample of **C-2**·12NO_3 in 26% yield.

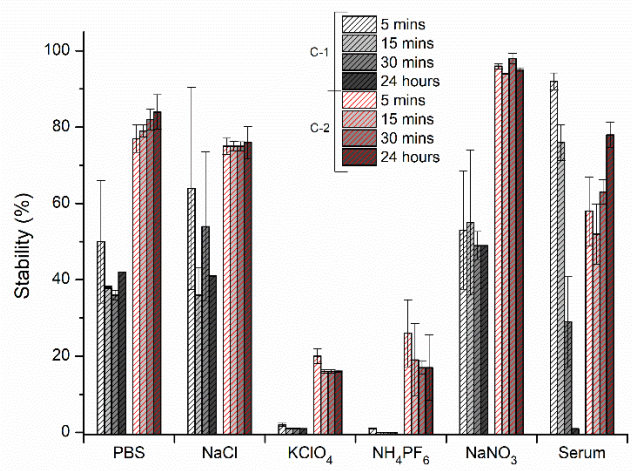

Figure 4. Stability of encapsulated complexes to different anions and conditions. 100 μM solution of salt was added to each cage made at their respective EC_{95} (100 μM for **C-1** and 1.9 μM for **C-2**). For details see Supporting Information.

Returning to radiochemical labelling experiments, we were delighted to find that substitution of the cage structure with 12 amino groups had an unforeseen yet very positive impact on [^{99m}Tc]TcO_4^- encapsulation. In the absence of competing anions, the concentration of **C-2** required to achieve >95% RCY was reduced to 1.9 μM, nearly 50-fold lower than **C-1**, with an EC_{50} value of just 0.05 μM (Figure 3, red circles). Furthermore, repeating the same anion displacement experiments with **C-2** showed that this increase in affinity is specific to

[^{99m}Tc]TcO_4^-, as higher stability is observed even with a much greater mole ratio of competing anions (Figure 4, red bars). Most significantly, however, we were gratified to see that the presence of serum gave no discernible drop in radiochemical stability over 24 hours, indicating that the amino groups have the desired effect of increasing cage robustness. This improved stability also correlates with a lack of reactivity towards glutathione (Figure S7).

In light of the improved serum stability and lower dose required to fully encapsulate [^{99m}Tc]TcO_4^-, **C-2** was selected for *in vivo* SPECT imaging experiments. MTT assays revealed low cytotoxicity relative to administered dose (CC_{50} = 10.6 μM, see Supporting Information).[17] [^{99m}Tc]TcO_4^- is used clinically to measure thyroid function by replacing iodide in the sodium-iodide symporter (NIS). NIS is also expressed in some non-thyroidal tissues including salivary glands, lacrimal glands and stomach.[18] When [^{99m}Tc][TcO_4⊂**C-2**]$^{11+}$ was administered and imaged, a reproducible difference in biodistribution was observed, using multiple animals, separate radiolabelling reactions and also different synthetic batches of cage (Figure 5 and S12), with significant uptake noted in the liver. These imaging results are consistent with the radiochemical stability data, in which a small amount of pertechnetate is displaced with blood-based anions, causing some NIS mediated thyroid and stomach uptake. Liver uptake vs. renal clearance was unexpected and is usually attributed to macrophage uptake of larger nano-sized species. In the case of [^{99m}Tc][TcO_4⊂**C-2**]$^{11+}$, the positive external charge and well defined molecular shape may result in protein binding influencing the liver uptake.[19] However, liver uptake also provides compelling evidence that the capsule remains intact during imaging, as disassembly would destroy the high affinity cavity that keeps the anion associated with the cage in the presence of a vast excess of biological cations. Extraction of liver tissue gave a sample with ca. 30% of the [^{99m}Tc]TcO_4^- anion associated with the host, with the remainder released (as pertechnetate) during the extraction process. The radioactivity associated with the host could then be quantitatively released as [^{99m}Tc]TcO_4^- by the addition of acetonitrile (see Supporting Information). *Ex vivo* biodistribution studies were carried out post-imaging to quantify uptake in various organs at a single time-point (Figure S11). Consistent with the SPECT images, the most significant uptake was noted in the thyroid (18.77% ID/g), liver (16.52% ID/g) and stomach (38.96% ID/g) (full biodistribution graphs are presented in Figure S13).

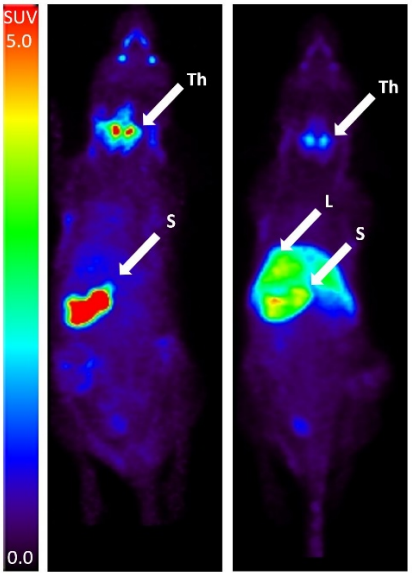

Figure 5. Comparison of [^{99m}Tc]TcO_4^- uptake in naïve mice (left) vs. [^{99m}Tc][TcO_4⊂**C-2**]$^{11+}$ (right). Free [^{99m}Tc]TcO_4^- was injected into a naïve anaesthetised animal 40 minutes prior to a 20 minute SPECT acquisition. Caged [^{99m}Tc]TcO_4^- was injected into a naïve anaesthetised animal 20 minutes prior to a 100 minute SPECT acquisition. Encapsulation results in reduced thyroid and stomach uptake, and increased liver uptake. Images are maximum intensity coronal projections. Additional examples are provided in the Supporting Information. S=Stomach, Th = Thyroid, L=Liver.

While the (pre)clinical use of self-assembled carrier systems is still in its infancy, we have demonstrated a clear step forward, showing both the robustness of a $Co^{III}_4L_6$ cage *in vivo* and that binding the [^{99m}Tc]TcO_4^- anion significantly affects its biodistribution. While this perturbation almost certainly arises due to a difference in size and charge, the potential to modify the cage exterior for targeted molecular-delivery is clear, most obviously utilizing the amino groups for conjugation with peptides or other biologically relevant targeting groups.[20] While we are currently optimising this radiolabel encapsulation approach, to reduce the amount of "cold" precursor required, this method provides a clear benefit both in terms of simplicity and speed. While the decay of [^{99m}Tc]TcO_4^- is relatively slow, we anticipate this could be very advantageous for some of the shorter lived PET isotopes.[21] Consequently, we foresee that this or similar systems could act as a universal platform for multiple imaging modalities and be expanded to the delivery of radiotherapeutic isotopes including rhenium-188.[22]

ASSOCIATED CONTENT

Supporting Information

The Supporting Information is available free of charge on the ACS Publications website. This includes synthetic details and characterization, binding constant and kinetic experiments, details of radiochemical yield determination, stability, MTT assays and SPECT imaging experiments.

AUTHOR INFORMATION

Corresponding Authors

Paul.Lusby@ed.ac.uk, S.J.Archibald@hull.ac.uk

Author Contributions

§These authors contributed equally.

Notes

The authors declare no competing financial interests.

ACKNOWLEDGMENT

This work was supported by the EPSRC, The University of Edinburgh, The University of Hull and the Daisy Appeal charity (grant no. DAhul2011). We thank Dr Assem Allam and his family for the generous donation to help found the PET Research Centre at the University of Hull. We thank the EPSRC UK National Crystallography Service at the University of Southampton for the collection of the crystallographic data.[23]

REFERENCES

(1) (a) Zolle, I. *Technetium-99m Pharmaceuticals: Preparation and Quality Control in Nuclear Medicine*; Springer: Berlin, Heidelberg, New York, **2007**. (b) Brenner, A. I.; Koshy, J.; Morey, J.; Lin, C.; DiPoce, J., *Semin. Nucl. Med.* **2012**, *42*, 11. (c) Jain, D., *Semin. Nucl. Med.* **1999**, *29*, 221. (d) *Suga, K. Ann. Nucl. Med.* **2002**, *16*, 303.

(2) (a) Dondi, M.; Pascual, T.; Paez, D.; Einstein, A. J. *Am. J. Cardiovasc. Drugs* **2017**, *17*, 441. (b) Jurgens, S.; Herrmann, W. A.; Kuhn, F. E., *J. Organomet. Chem.* **2014**, *751*, 83. (c) Kniess, T.; Laube, M.; Wust, F.; Pietzsch, J., *Dalton Trans.* **2017**, *46*, 14435.

(3) (a) Liu, S. *Chem. Soc. Rev.* **2004**, *33*, 445. (b) Bartholoma, M. D.; Louie, A. S.; Valliant, J. F.; Zubieta, J. *Chem. Rev.* **2010**, *110*, 2903. (c) Nakai, M.; Pan, J. H.; Lin, K. S.; Thompson, J. R.; Nocentini, A.; Supuran, C. T.; Nakabayashi, Y.; Storr, T. *J. Inorg. Biochem.* **2018**, *185*, 63-70. (d) Burke, B. P.; Seemann, J.; Archibald, S. J., *Advances in Inorganic Chemistry, Vol 68: Insights from Imaging in Bioinorganic Chemistry*, VanEldik, R.; Hubbard, C. D., Eds. **2016**; Vol. 68, pp 301-339.

(4) (a) Katayev, E. A.; Kolesnikov, G. V.; Sessler, J. L. *Chem. Soc. Rev.* **2009**, *38*, 1572. (b) Banerjee, D.; Kim, D.; Schweiger, M. J.; Kruger, A. A.; Thallapally, P. K., *Chem. Soc. Rev.* **2016**, *45*, 2724. (c) Farrell, D.; Gloe, K.; Gloe, K.; Goretzki, G.; McKee, V.; Nelson, J.; Nieuwenhuyzen, M.; Pal, I.; Stephan, H.; Town, R. M.; Wichmann, K. *Dalton Trans.* **2003**,1961.

(5) (a) Fleming, J. S.; Mann, K. L. V.; Carraz, C.-A.; Psillakis, E.; Jeffery, J. C.; McCleverty, J. A.; Ward, M. D. *Angew. Chem. Int. Ed.* **1998**, *37*, 1279. (b) Glasson, C. R. K.; Clegg, J. K.; McMurtrie, J. C.; Meehan, G. V.; Lindoy, L. F.; Motti, C. A.; Moubaraki, B.;. Murray, K. S.; Cashion, J. D. *Chem. Sci.* **2011**, *2*, 540. (c) Custelcean, R.; Bonnesen, P. V.; Duncan, N. C.; Zhang, X.; Watson, L.; Van Berkel, G.; Parson, W. B.; Hay, B. P. *J. Am. Chem. Soc.* **2012**, *134*, 8525. (d) Zhang, D.; Ronson, T. K.; Mosquera, J.; Martinez, A.; Guy, L.; Nitschke, J. R. *J. Am. Chem. Soc.* **2017**, *139*, 6574.

(6) Burke B. P., Cawthorne C., Archibald S.J. Chapter 23: Radionuclide Labelling and Imaging of Magnetic Nanoparticles. In Clinical Applications of Magnetic Nanoparticles ed. Nguyen Thanh, *Taylor and Francis*, London, 2018, pp 411-430.

(7) (a) Yoshizawa, M.; Klosterman, J. K.; Fujita, M. *Angew. Chem. Int. Ed.* **2009**, *48*, 3418. (b) Chakrabarty, R.; Mukherjee, P. S.; Stang, P. J. *Chem. Rev.* **2011**, *111*, 6810. (c) Ward, M. D.; Raithby, P. R. Chem. Soc. Rev. **2013**, *42*, 1619. (d) Cook, T. R.; Stang, P. J. *Chem. Rev.* **2015**, *115*, 7001; (e) Brown, C. J.; Toste, F. D.; Bergman, R. G.; Raymond, K. N., *Chem. Rev.*, **2015**, *115*, 3012. (f) Zarra, S.; Wood, D. M.; Roberts, D. A.; Nitschke, J. R. *Chem. Soc. Rev.* **2015**, *44*, 419. (g) Saha, M. L.; Yan, X.; Stang, P. J. *Acc. Chem. Res.* **2016**, *49*, 2527. (h) Bloch, W. M.; Clever, G. H. *Chem. Commun.*, **2017**, *53*, 8506.

(8) (a) Kang, J.; Rebek Jr., J. *Nature* **1997**, *385*, 50. (b) Yoshizawa, M.; Tamura, M.; Fujita, M. *Science* **2006**, *312*, 251. (c) Pluth, M. D.; Bergman, R. G.; Raymond, K. N. *Science* **2007**, *316*, 85. (d) Lee, S. J.; Cho, S.-H.; Mulfort, K. L.; Tiede, D.M.; Hupp, J. T.; Nguyen, S. T. *J. Am. Chem. Soc.* **2008**, *130*, 16828. (e) Hastings, C. J.; Pluth, M. D.; Bergman, R. G.; Raymond, K. N. *J. Am. Chem. Soc.* **2010**, *132*, 6938. (f) Bolliger, J. L.; Belenguer, A. M.; Nitschke, J. R. *Angew. Chem. Int. Ed.* **2013**, *52*, 7958. (g) Kaphan, D. M.; Levin, M. D.; Bergman, R. G.; Raymond, K. N.; Toste, F. D. *Science* **2015**, *350*, 1235. (h) Zhang, Q.; Tiefenbacher, K. *Nat. Chem.* **2015**, *7*, 197. (i) Cullen, W.; Misuraca, M. C.; Hunter, C. A.; Williams, N. H.; M. D. Ward, *Nat. Chem.* **2016**, *8*, 231. (j) Wang, Q.-Q.; Gonell, S.; Leenders, S. H. A. M.; Dürr, M.; Ivanović-Burmazović, I.; Reek, J. N. H. *Nat. Chem.* **2016**, *8*, 225. (k) Omagari, T.; Suzuki, A.; Akita, M.; Yoshizawa, M. *J. Am. Chem. Soc.* **2016**, *138*, 499. (l) Martí-Centelles, V.; Lawrence, A. L.; Lusby, P. J. *J. Am. Chem. Soc.* **2018**, 140, 2862. (m) Holloway, L. R.; Bogie, P. M.; Lyon, Y.; Ngai, C.; Miller, T. F.; Julian, R. R.; Hooley, R. J. *J. Am. Chem. Soc.* **2018**, *140*, 8078.

(9) Paul, L. E. H.; Therrien, B.; Furrer, J. *Inorg. Chem.* **2012**, *51*, 1057.

(10) For a recent review, see (a) Cook, T. R.; Vajpayee, V.; Lee, M. H.; Stang, P. J.; Chi, K. W. Acc. Chem. Res. **2013**, *46*, 2464. For various examples, see (b) Pascu, G. I.; Hotze, Anna C. G.; Sanchez-Cano, C.; Kariuki, B. M.; Hannon, M. J. *Angew. Chem. Int. Ed.* **2007**, *46*, 4374. (c) Kieltyka, R.; Englebienne, P.; Fakhoury, J.; Autexier, C.; Moitessier, N.; Sleiman, H. F. *J. Am. Chem. Soc.* **2008**, *130*, 10040. (d) Faulkner, A. D.; Kaner, R. A.; Abdallah, Q. M. A.; Clarkson, G.; Fox, D. J.; Gurnani, P.; Howson, S. E.; Phillips, R. M.; Roper, D. I.; Simpson, D. H.; Scott, P. *Nature Chem.* **2014**, *6*, 797. (e) McNeill, S. M.; Preston, D.; Lewis, J. E. M.; Robert, A.; Knerr-Rupp, K.; Graham, D. O.; Wright, J. R.; Giles, G. I.; Crowley, J. D. *Dalton Trans.* **2015**, *44*, 11129. (f) Garci, A.; Castor, K. J.; Fakhoury, J.; Do, J. L.; Di Trani, J.; Chidchob, P.; Stein, R. S.; Mittermaier, A. K.; Friščić, T.; Sleiman, H. *J. Am. Chem. Soc.* **2017**, *139*, 16913. (g) Zhou, J.; Zhang, Y.; Yu, G.; Crawley, M. R.; Fulong, C. R. P.; Friedman, A. E.; Sengupta, S.; Sun, J.; Li, Q. Huang, F.; Cook, T. R. *J. Am. Chem. Soc.* **2018**, *140*, 7730.

(11) (a) Therrien, B.; Suess-Fink, G.; Govindaswamy, P.; Renfrew, A. K.; Dyson, P. J. *Angew. Chem. Int. Ed.* **2008**, *47*, 3773. (b) Lewis, J. E. M.; Gavey, E. L.; Cameron, S. A.; Crowley, J. D. *Chem. Sci.* **2012**, *3*, 778. (c) Zheng, Y.-R.; Suntharalingam, K.; Johnstone, T. C.; Lippard, S. J. *Chem. Sci.* **2015**, *6*, 1189. (d) Ahmedova, A.; Mihaylova, R.; Momekova, D.; Shestakova, P.; Stoykova, S.; Zaharieva, J.; Yamashina, M.; Momekov, G.; Akita, M. Yoshizawa, M. *Dalton Trans.* **2016**, *45*, 13214. (e) Schmidt, A.; Molano, V.; Hollering, M.; Pöthig, A.; Casini, A.; Kühn, F. E. *Chem. Eur. J.* **2016**, *22*, 2253. (f) Rodríguez, J.; Mosquera, J.; Couceiro, J. R.; Nitschke, J. R.; Vázquez, M. E.; Mascareñas, J. L. *J. Am. Chem. Soc.* **2017**, 139, 55. (g) Samanta, S. K.; Quigley, J.; Vinciguerra, B.; Briken, V.; Isaacs, L. *J. Am. Chem. Soc.* **2017**, *139*, 9066. (h) D., S.; Misra, S. K.; Saha, M. L.; Lahiri, N.; Louie, J.; Pan, D.; Stang, P. J. *Proc. Natl. Acad. Sci.* **2018**, *115*, 8087. (i) Mosquera, J.; Henriksen-Lacey, M.; García, I.; Martínez-Calvo, M.; Rodríguez, J.; Mascareñas, J. L.; Liz-Marzán, L. M. *J. Am. Chem. Soc.* **2018**, *140*, 4469.

(12) (a) Grishagin, I. V.; Pollock, J. B.; Kushal, S.; Cook, T. R.; Stang, P. J.; Olenyuk, B. Z. *Proc. Natl Acad. Sci. USA* **2014**, *111*, 18448. (b) Yu, G.; Zhang, M.; Saha, M. L.; Mao, Z.; Chen, J.; Yao, Y.; Zhou, Z.; Liu, Y.; Gao, C.; Huang, F.; Chen, X. Stang, P. J. *J. Am. Chem. Soc.* **2017**, *139*, 15940.

(13) (a) Symmers, P. R.; Burke, M. J.; August, D. P.; Thomson, P. I. T.; Nichol, G. S.; Warren, M. R.; Campbell, C. J.; Lusby, P. J. *Chem. Sci.* **2015**, *6*, 756. (b) Burke, M. J.; Nichol, G. S.; Lusby, P. J. *J. Am. Chem. Soc.* **2016**, *138*, 9308.

(14) Bennink, R. J.; van den Elzen, B. D.; Kuiken, S. D.; Boeckxstaens, G. E. *J. Nucl. Med.* **2004**, *45*, 147. (b) Connolly, L. P.; Treves, S. T.; Bozorgi, F.; O' Connor, S. C., *J. Nucl. Med.* **1998**, *39*, 1458. (c) Fruhwirth, G. O.; Diocou, S.; Blower, P. J.; Ng, T.; Mullen, G. E. D. *J. Nucl. Med.* **2014**, *55*, 686.

(15) (a) Hristova, Y. R.; Smulders, M. M. J.; Clegg, J. K.; Breiner B.; Nitschke, J. R. *Chem. Sci.* **2011**, *2*, 638. (b) Zhang, D.; Ronson, T.K.; Mosquera, J.; Martinez, A.; Guy, L.; Nitschke, J. R. *J. Am. Chem. Soc.* **2017**, *139*, 6574.

(16) Ahmedova, A.; Mihaylova, R.; Momekova, D.; Shestakova, P.; Stoykova, S.; Zaharieva, J.; Yamashina, M.; Momekov, G.; Akita, M.; Yoshizawa, M. Dalton Trans. **2016**, *45*, 13214.
(17) For *in vivo* work, the concentration of **C-2** required to remain >90% radiochemical stability *in vivo* was used. This total administered cage dose of 40 μg (1 mg/kg for a 40g mouse) corresponds to 3.1 μg of cobalt (0.08 mg cobalt/kg).
(18) (a) Chen, C. C.; Holder, L. E.; Scovill, W. A.; Tehan, A. M.; Gann, D. S. *J. Nucl. Med.* **1997**, *38*, 834. (b) Jiang, H. L.; DeGrado, T. R. *Theranostics* **2018**, *8*, 3918.
(19) (a) Gustafson, H. H.; Holt-Casper, D.; Grainger, D. W.; Ghandehari, H. *Nano Today* **2015**, *10*, 487. (b) Kiessling, F.; Mertens, M. E.; Grimm, J.; Lammers, T., *Radiology* **2014**, *273*, 10. (c) Aoyama, M.; Hata, K.; Higashisaka, K.; Nagano, K.; Yoshioka, Y.; Tsutsumi, Y., *Biochem. Biophys. Res. Commun.* **2016**, *480*, 690. (d) Mortimer, G. M.; Butcher, N. J.; Musumeci, A. W.; Deng, Z. J.; Martin, D. J.; Minchin, R. F. *Acs Nano* **2014**, *8*, 3357-3366. (e) Burke, B. P.; Baghdadi, N.; Kownacka, A. E.; Nigam, S.; Clemente, G. S.; Al-Yassiry, M. M.; Domarkas, J.; Lorch, M.; Pickles, M.; Gibbs, P.; Tripier, R.; Cawthorne, C.; Archibald, S. J., *Nanoscale* **2015**, *7*, 14889.
(20) (a) Liu, S. *Adv. Drug Del. Rev.* **2008**, *60*, 1347. (b) Fani, M.; Maecke, H. R. *Eur. J. Nucl. Med. Mol. Imag.* **2012**, *39*, 11. (c) Mewis, R. E.; Archibald, S. J. *Coord. Chem. Rev.* **2010**, *254*, 1686. (d) Pimlott, S. L.; Sutherland, A. *Chem. Soc. Rev.* **2011**, *40*, 149. (e) Schottelius, M.; Wester, H. J. *Methods* **2009**, *48*, 161. (f) Storr, T.; Thompson, K. H.; Orvig, C. *Chem. Soc. Rev.* **2006**, *35*, 534.
(21) (a) Ge, H.; Riss, P. J.; Mirabello, V.; Calatayud, D. G.; Flower, S. E.; Arrowsmith, R. L.; Fryer, T. D.; Hong, Y.; Sawiak, S.; Jacobs, R. M. J.; Botchway, S. W.; Tyrrell, R. M.; James, T. D.; Fossey, J. S.; Dilworth, J. R.; Aigbirhio, F. I.; Pascu, S. I. *Chem* **2017**, *3*, 437. (b) Wadas, T. J.; Wong, E. H.; Weisman, G. R.; Anderson, C. J. *Chem. Rev.* **2010**, *110*, 2858. (c) Burke, B. P.; Clemente, G. S.; Archibald, S. J. *J. Label. Compd. Radiopharm.* **2014**, *57*, 239.
(22) (a) Blower, P. *Dalton Trans.* **2006**, 1705. (b) Knapp, F. F. *Cancer Biother. Radiopharm.* **1998**, *13*, 337. (c) van Dodewaard-de Jong, J. M.; de Klerk, J. M. H.; Bloemendal, H. J.; Oprea-Lager, D. E.; Hoekstra, O. S.; van den Berg, H. P.; Los, M.; Beeker, A.; Jonker, M. A.; O'Sullivan, J. M.; Verheul, H. M. W.; van den Eertwegh, A. J. M. *Eur. J. Nucl. Med. Mol. Imag.* **2017**, *44*, 1319. (d) Baum, R. P.; Kulkarni, H. R. *Theranostics* **2012**, *2*, 437.
(23) Coles, S.J.; Gale, P.A., *Chem. Sci.* **2012**, *3*, 683.

Table of Contents (TOC) graphic: